

The control of pigment cell pattern formation in the California newt, *Taricha torosa*

R. P. TUCKER* AND C. A. ERICKSON†

Department of Zoology, University of California, Davis, CA 95616, USA

SUMMARY

Neural crest-derived pigment cells form species-specific patterns of pigmentation in amphibian embryos. We have characterized the appearance and changes in pigment cell distribution in the embryos of the California newt, *Taricha torosa*. Black melanophores first appear scattered over the surface of the somites intermingled with yellow xanthophores in stage 34/35 embryos. The melanophores then migrate either dorsally to form a dorsal stripe at the apex of the somites or ventrally along the intersomitic furrows to form a midbody stripe at the somite–lateral plate mesoderm border. Xanthophores remain between the two melanophore stripes and are also found in the dorsal fin and head. The formation of the dorsal stripe coincides with a change in melanophore tissue affinity from the surface of the somites to the subectodermal extracellular matrix (ECM). The latter substratum is the location of the cue used to organize the dorsal stripe. In addition, melanophores become elongate and highly arborized, which would allow them to extend to the region where the dorsal stripe forms. In contrast, xanthophores do not form long processes *in vitro*. This suggests that the ability of melanophores but not xanthophores to search for a cue at the apex of the somites may account in part for the segregation of these cell types. Melanophores and xanthophores are trapped to form the midbody stripe by the pronephric duct, which is located just beneath the ectoderm at the bases of the intersomitic furrows. Ablation of the duct prevents formation of the midbody stripe, although melanophores and xanthophores still fail to migrate ventrally over the lateral plate mesoderm. Melanophores grafted to the ventral midline fail to leave the confines of the donor tissue. This suggests that a factor in the lateral plate mesoderm in addition to the pronephric duct is inhibiting further ventral migration. There is no gross morphological difference in the organization of the subectodermal ECM dorsal and ventral to the pronephric duct as revealed by alcian blue, ruthenium red and staining with antibodies to fibronectin. We also conclude that the directed dispersal of the neural crest into the space between the somites and ectoderm is due to contact inhibition of cell movement, since *T. torosa* neural crest cells demonstrate contact inhibition *in vitro* and there are enough cells in the lateral migratory spaces to make contact events likely during dispersal.

INTRODUCTION

The trunk neural crest is a transient population of mesenchymal cells that appears near the dorsal surface of the neural tube soon after neurulation is complete. In amphibian embryos, these cells migrate from their site of origin along three major pathways: dorsally, into the expanding dorsal fin; ventrally, between the somites and the neural tube; and laterally, between the ectoderm and the

* Present address: Friedrich Miescher-Institut, PO Box 2543, CH-4002 Basel, Switzerland.

† Author for reprints.

Key words: neural crest, pigment cells, contact inhibition, extracellular matrix, *Taricha torosa*.

somites (for reviews see Hörstadius, 1950; Weston, 1980; Le Douarin, 1982; Erickson, 1986).

Among the derivatives of the amphibian neural crest are three types of pigment cells (DuShane, 1935; Stevens, 1954): black or brown melanophores; yellow xanthophores; and iridophores, which contain reflective organelles (see Bagnara *et al.* 1979; Frost, Epp & Robinson, 1984a,b). These cells become localized in the embryonic dermis to form species-specific patterns of pigmentation.

There is a substantial literature on the development of pigment cell patterns in the three species of newts belonging to the genus *Taricha* (formerly *Triturus*). *Taricha torosa*, the California newt, has two melanophore stripes. A dorsal stripe runs along the base of the dorsal fin and a second, less distinct, stripe is found at the somite-lateral plate mesoderm border. *T. granulosa* also has a black dorsal stripe, but, unlike *T. torosa*, melanophores are found ventrally over the surface of the lateral plate mesoderm. This pattern resembles the distribution of melanophores in the European newt *Triturus alpestris* (Epperlein, 1982; Epperlein & Claviez, 1982a,b). Finally, *Taricha rivularis* lacks melanophore stripes altogether. Instead, the melanophores remain as individual cells scattered over the surface of the somites and the dorsal portion of the yolk mass.

Twitty (1936, 1944, 1945, 1953) and his colleagues (Twitty & Bodenstein, 1939, 1944; Twitty & Niu, 1948, 1954) attempted to determine what aspects of the species-specific melanophore patterns in *T. torosa*, *T. rivularis* and *T. granulosa* are controlled by environmental influences (e.g. regions of differential adhesion or regional control of melanophore differentiation) and to what extent differences in the melanophores themselves can account for pattern formation in a series of hybridization, grafting and tissue culture experiments. In brief, Twitty and his associates concluded that formation of the dorsal stripe of melanophores found in *T. torosa* and *T. granulosa* but not *T. rivularis* is the result of differences in the adhesive properties of the melanophores in these three species and not their environment. For example, melanophores from *T. rivularis* do not form stripes when orthotopically grafted into *T. torosa*, whereas *T. torosa* melanophores form a dorsal stripe when *T. rivularis* is the host. These results were supported with tissue culture experiments conducted by Twitty & Bodenstein (1939), who observed that *T. torosa* melanophores form clusters in culture, whereas melanophores from *T. rivularis* do not. In contrast, the midbody melanophore stripe found only in *T. torosa* is due to an environmental cue, since neither *T. rivularis* nor *T. granulosa* melanophores migrate ventrally over the yolk in *T. torosa*, and *T. torosa* melanophores migrate over the yolk mass in the other two species. Twitty (1936) hypothesized that the cue responsible for the formation of the midbody stripe in *T. torosa* is the abrupt angle taken by the ectoderm and lateral plate mesoderm as it begins to surround the bulging yolk mass. Finally, Twitty & Niu (1948, 1954) concluded from a series of *in vitro* experiments that the dispersal of pigment cells from the neural tube is the result of negative chemotaxis.

We have reexamined these conclusions using methods that were not available to earlier researchers in order to determine the mechanisms underlying pigment cell

pattern formation in the California newt, *T. torosa*. These techniques, which include the identification of weakly pigmented xanthophores *in situ* by fluorescence microscopy, histological and immunocytochemical localization of extracellular matrix (ECM) components, time-lapse videomicroscopy and electron microscopy, have permitted us to elucidate the mechanisms of dorsal and midbody melanophore stripe formation, the segregation of different types of pigment cells and the dispersal of pigment cell precursors from their site of origin.

MATERIALS AND METHODS

Taricha torosa torosa (Twitty, 1942) egg clusters were collected from ponds in the San Francisco Bay area. Embryos were removed from their gelatinous integuments using a razor blade, and the fertilization envelopes were removed with tungsten needles. Embryos were raised in either 20 % Steinberg's solution or tap water at 16°C. The animals were staged using the development tables of Schreckenberg & Jacobson (1975).

Videomicrography of melanophore pattern development

The appearance and changes in the distribution of melanophores were observed using a Nikon Diaphot inverted microscope with illumination provided by a substage fibre optics light source (Dyomics). Embryos were rinsed in 20 % Steinberg's solution and anaesthetized with a few crystals of ethyl m-aminobenzoate (MS-222; Sigma). For videomicrography, it was necessary to restrain the animals to prevent ciliary gliding movement. This was accomplished by gently placing the head and tail of the embryo into appropriately sized fire-polished capillary tubes. During the video recording, the embryos were kept at room temperature (22°C) to increase the rate of development. Time-lapse video recordings were made with an RCA or MTI videocamera and a Panasonic 8050 VHS videocassette player. Rates of cell movement and patterns of migration were analysed by tracing cell positions on acetate sheets placed over the display of a black and white monitor (Audiotronics).

Patterns of migration were also recorded by 35 mm photography. Photographs were taken at 3 h intervals over a 72 h period with Tri-X (Kodak) black and white film using a Nikon FE camera. Still photography was in some respects superior to videomicrography for recording cell behaviour *in vivo* over extended periods, because constant illumination 'bleached' the pigmentation of melanophores, making it difficult to resolve cell morphology.

Identification of pigment cells

Melanophores were identified as black or grey cells in living embryos, whole mounts and sections for light microscopy. In the transmission electron microscope (TEM) melanophores were identified by the presence of characteristic electron-dense melanosomes (see below).

The distribution of xanthophores was determined by NH_4OH -induced autofluorescence using techniques described previously (Epperlein & Claviez, 1982a; Tucker, 1986). In brief, embryos were anaesthetized in MS-222 and immersed in 10 % NH_4OH . Specimens were then mounted on a glass slide and viewed with a Zeiss epifluorescence microscope. Immediate observation was necessary since the embryos disintegrated within 15 min of NH_4OH treatment. The autofluorescence of pteridines results in xanthophores appearing bluish white when viewed with appropriate filters (365 nm excitation, 395 nm barrier). This technique is specific for xanthophores since in older embryos only externally visible yellow cells fluoresced.

Iridophores were identified in plastic-embedded whole mounts (see below) as lustrous silver cells visible when viewed under bright oblique illumination.

Light and electron microscopy

Embryos (stages 16 to 40+) were embedded in plastic for whole-mount preparations as well as thick and thin sectioning. For whole mounts and light microscopy, specimens were fixed in 2 %

glutaraldehyde in 0.1 M-sodium cacodylate buffer for 2 to 4 h at room temperature or overnight at 4°C. Specimens were then rinsed in buffer, dehydrated in ethanol, and infiltrated and embedded in Epon-Araldite. For electron microscopy, specimens were postfixed in 1 % OsO₄ in sodium cacodylate buffer for 30 min at room temperature following the buffer rinse. Specimens were either sectioned at 5 µm on a Sorvall MT-2 microtome and stained in drops of 0.05 % toluidine blue, or thin sectioned on a Reichert Om U3 ultramicrotome, stained with uranyl acetate and lead citrate, and observed at 60 kV or 80 kV in a Philips 410 TEM.

Some embryos (n = 12, stages 36 to 40) were prepared for scanning electron microscopy (SEM). Specimens were fixed in 2 % glutaraldehyde in sodium cacodylate buffer overnight at 4°C, rinsed in buffer, and photographed. Embryos were then transferred to wax dishes, pinned, and a rectangular piece of ectoderm was removed with tungsten needles from the side of the embryo. Both the ectoderm and the remainder of the embryo were photographed, dehydrated in ethanol and critical-point dried with CO₂ in a Samdri-780A (Tousimis) critical-point drying apparatus. Specimens were then mounted on aluminium stubs with silver paint, sputter coated (Denton) with gold and observed at 20 kV in a Philips 501 SEM.

Identification of glycosaminoglycans

The distribution of glycosaminoglycans (GAG) was determined using alcian blue staining of paraffin sections and ruthenium red staining of embryos prepared for TEM using methods described in detail elsewhere (Turley, Erickson & Tucker, 1985; Tucker, 1986; Tucker & Erickson, 1986b). For alcian blue staining, embryos (n = 7, stages 32 to 40) were fixed overnight in 10 % formaldehyde with or without 0.5 % cetylpyridinium chloride (CPC; Polysciences; see Derby & Pintar, 1978) at room temperature, dehydrated in ethanol, cleared in xylene, and infiltrated and embedded in Paraplast (Lancer). Embryos were serially sectioned at 7 µm, rehydrated, treated with 5 M-HCl for 30 s and stained in 1 % alcian blue 8G-X (MCB) in 0.025 M-MgCl₂ (pH 2.6) overnight. Stained sections were then rinsed, dehydrated, cleared in xylene, and mounted in Permount (Fisher). For ruthenium red staining, embryos (n = 5, stages 38 to 40) were fixed in 2 % glutaraldehyde with 0.1 % ruthenium red (Polysciences, see Luft, 1971) and 0.1 % tannic acid (Fisher) in PBS at 4°C. After 30 min, specimens were cut transversely, approximately in half, with a razor blade to facilitate penetration of the fixative and stains, and the specimens were kept in the fixative overnight at 4°C. Embryos were then rinsed in 0.1 M-sodium cacodylate buffer, postfixed in 1 % OsO₄ for 30 min at room temperature (if stain was present in the fixative, ruthenium red was also present in the postfixative), rinsed in double-distilled H₂O and further prepared for thin sectioning as outlined above. Thin sections were made following thick sectioning of the specimen to a point approximately 50 µm from the cut surface. The types of GAG stained were determined by digestion of the matrix with chondroitinase ABC (Seikagaku Kogyo) or *Streptomyces* hyaluronidase (Seikagaku Kogyo) using methods modified from Hay & Meier (1974) and reported in detail elsewhere (Tucker, 1986).

Immunocytochemistry

Stage 39/40 *T. torosa* embryos were fixed in Carnoy fixative for 4 h at room temperature, embedded in OCT compound (Miles) and frozen in 2-methyl butane cooled with dry ice. 10 µm sections were cut using a Bright cryostat, air dried, and rinsed three times in phosphate-buffered saline (PBS) and once in PBS with 0.5 % bovine serum albumin (BSA, Sigma). Sections were then incubated in anti-*Xenopus* plasma fibronectin (FN) anti-sera (1:40; a gift from C. C. Wylie and R. O. Hynes, see Heasman *et al.* 1981) for 1 h at room temperature. Following incubation with the primary antibody, sections were rinsed in PBS and incubated in goat anti-rabbit secondary antibody conjugated with FITC for 30 min at room temperature, rinsed and mounted in glycerol. Some sections were incubated in PBS-BSA for 1 h instead of primary anti-sera before incubation in secondary antibody to control for nonspecific background staining. Stained preparations were observed with a Leitz Dialux 20 epifluorescence microscope and photographed using a Leitz Vario-Orthomat camera.

Surgical manipulations

Ablation and grafting operations were carried out under sterile conditions on wax dishes in 100 % Steinberg's solution. To determine the effects of the ventral environment on melanophore differentiation and migratory behaviour, fragments of neural folds were grafted ventral to the pronephric duct and the resulting melanophore distribution was observed. Neural folds and the underlying neurectoderm were excised from the future anterior trunk region of stage 19 neurulae ($n = 3$) using tungsten needles. The prospective neural tissue was then grafted into a slit made in the ectoderm overlying the lateral plate mesoderm of an anaesthetized stage 23/24 host embryo. The grafted tissue was held in place until healed (approximately 30 min) using a fragment of a glass coverslip. The host embryo was then transferred to 20 % Steinberg's solution and monitored daily.

Pronephric duct primordia were removed from the right side of stage 22/23 embryos ($n = 5$) following procedures modified from Poole & Steinberg (1982). It was possible to remove completely the ovoid primordium without noticeably disturbing the underlying somites or removing the overlying ectoderm. After recording the development of melanophore and xanthophore patterns, presumably ductless larvae were embedded in plastic and sectioned at $5\text{ }\mu\text{m}$ (see above) to confirm the complete removal of the pronephric duct.

In vitro analysis of pigment cell behaviour and morphology

Detailed descriptions of *T. torosa* neural crest tissue culture methods have been presented elsewhere (Tucker & Erickson, 1986a,b). In brief, fragments of neural folds were excised with tungsten needles from stage 16/17 embryos and explanted onto tissue culture plastic dishes (Corning) containing half-strength ($\frac{1}{2}\times$) Leibovitz's L-15 medium (GIBCO) with antibiotics (gentamicin sulphate, Sigma; fungizone, GIBCO). To promote the differentiation of melanophores and xanthophores *in vitro*, 10 % foetal calf serum (FCS; GIBCO) was added to the medium. For other experiments, neural crest cells were cultured in $\frac{1}{2}\times$ L-15 saline alone or with $25\text{ }\mu\text{g ml}^{-1}$ plasma FN (BRL) added to the medium.

Some neural folds were cultured on top of collagen gels (see Elsdale & Bard, 1972; Tucker & Erickson, 1984). Eight parts collagen (Vitrogen 100; Collagen Corporation), 1 part $2\times$ L-15 medium and 1 part 0.142 N-NaOH were combined and diluted with $\frac{1}{2}\times$ L-15 with antibiotics (see above) and FCS. The final concentration of the collagen was approximately 6 %.

Contact behaviour was recorded using videomicroscopy (see above) with a Nikon Diaphot inverted phase-contrast microscope with an ice-chilled stage. Speed of movement was determined using methods described previously (Tucker & Erickson, 1984). In brief, nuclear displacement was traced on acetate sheets at 20 min intervals over a 2 h period. A Hipad Digitizer was used to enter the positional information into a computer to determine the rates of translocation on different substrata.

RESULTS

The development of melanophore patterns in *T. torosa* larvae can be separated into three phases: 'appearance' (stage 33/34), when the melanophores first become visible beneath the ectoderm in the lateral pathway; 'segregation' (stages 35 to 38), when the melanophores form the dorsal and midbody stripes; and the 'primary pattern' (stage 39/40), when melanophore motility wains and the dorsal stripe is accentuated by extensive branching of cell processes. The results of time-lapse analysis of melanophore pattern formation are described below.

Development of melanophore patterns

Melanophores become visible beneath the transparent ectoderm in *T. torosa* at stage 33/34 (Fig. 1A). The grey cells appear scattered over the surface of the

somites in the lateral pathway, where they have migrated from their site of origin on the neural tube.

As development proceeds, the scattered melanophores segregate into two populations: most of the cells move a short distance ($<200\ \mu\text{m}$) dorsally to form the dorsal stripe and others move ventrally to form the midbody stripe. The cells that move ventrally display rapid (up to $0.30\ \mu\text{m min}^{-1}$), highly directed motility until they reach the somite-lateral plate mesoderm border (Figs 1B,C, 2A). These cells are invariably following intersomitic furrows. 48 h after their initial appearance (Fig. 1D), the melanophores are found evenly spaced in the midbody stripe at the base of the furrows. This orderly arrangement is short-lived.

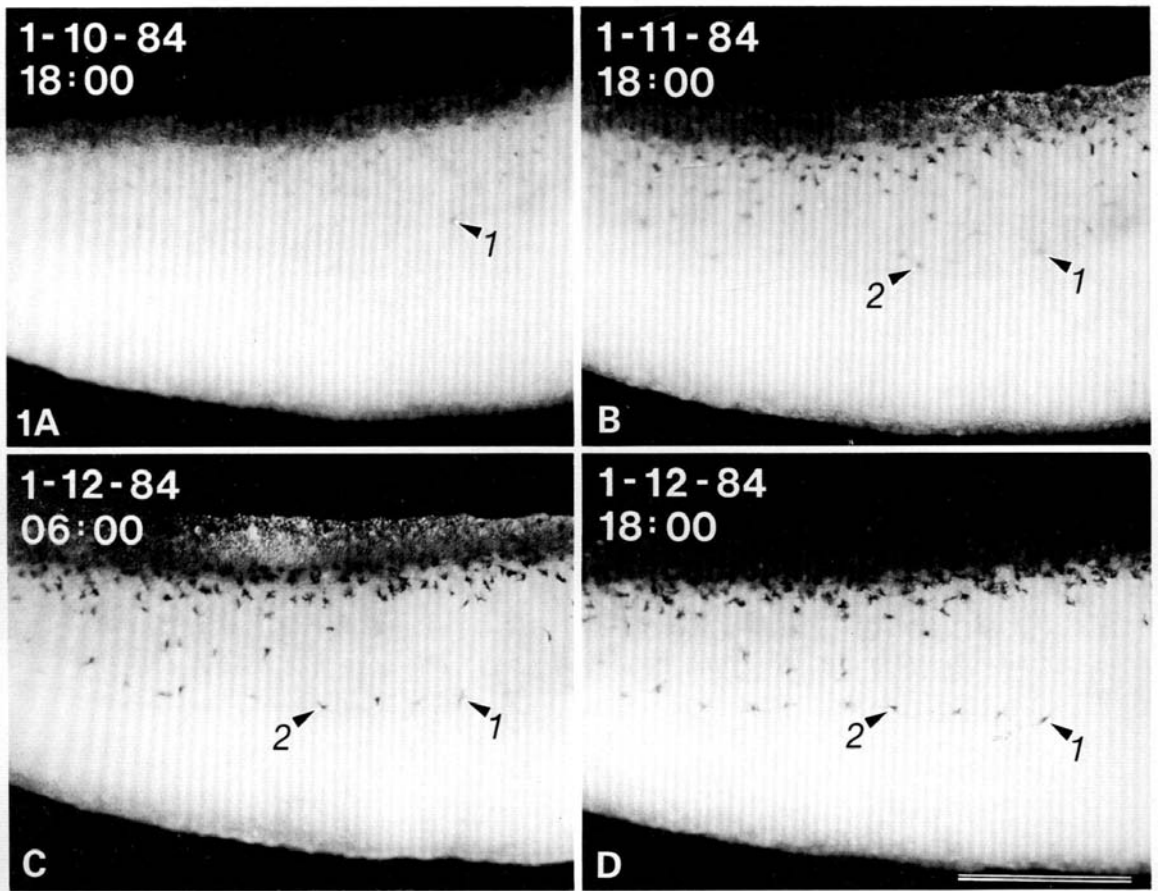


Fig. 1. Time-lapse analysis of melanophore pattern formation in *T. torosa*. (A) Melanophores first appear scattered over the surface of the somites at stage 34/35. The movements of melanophore 1 are shown in detail in Fig. 2A. (B) 24 h later, more melanophores have appeared, and the cells are more deeply pigmented. The movements of melanophore 2 are detailed in Fig. 2B. (C) 36 h after their appearance, the dorsal stripe and midbody stripe begin to become distinct. (D) After 48 h, melanophores (including cells 1 and 2) are found in the midbody stripe at the bases of the intersomitic furrows. Melanophores remaining between the midbody and dorsal stripes are found in the intersomitic furrows. Bar, 1 mm.

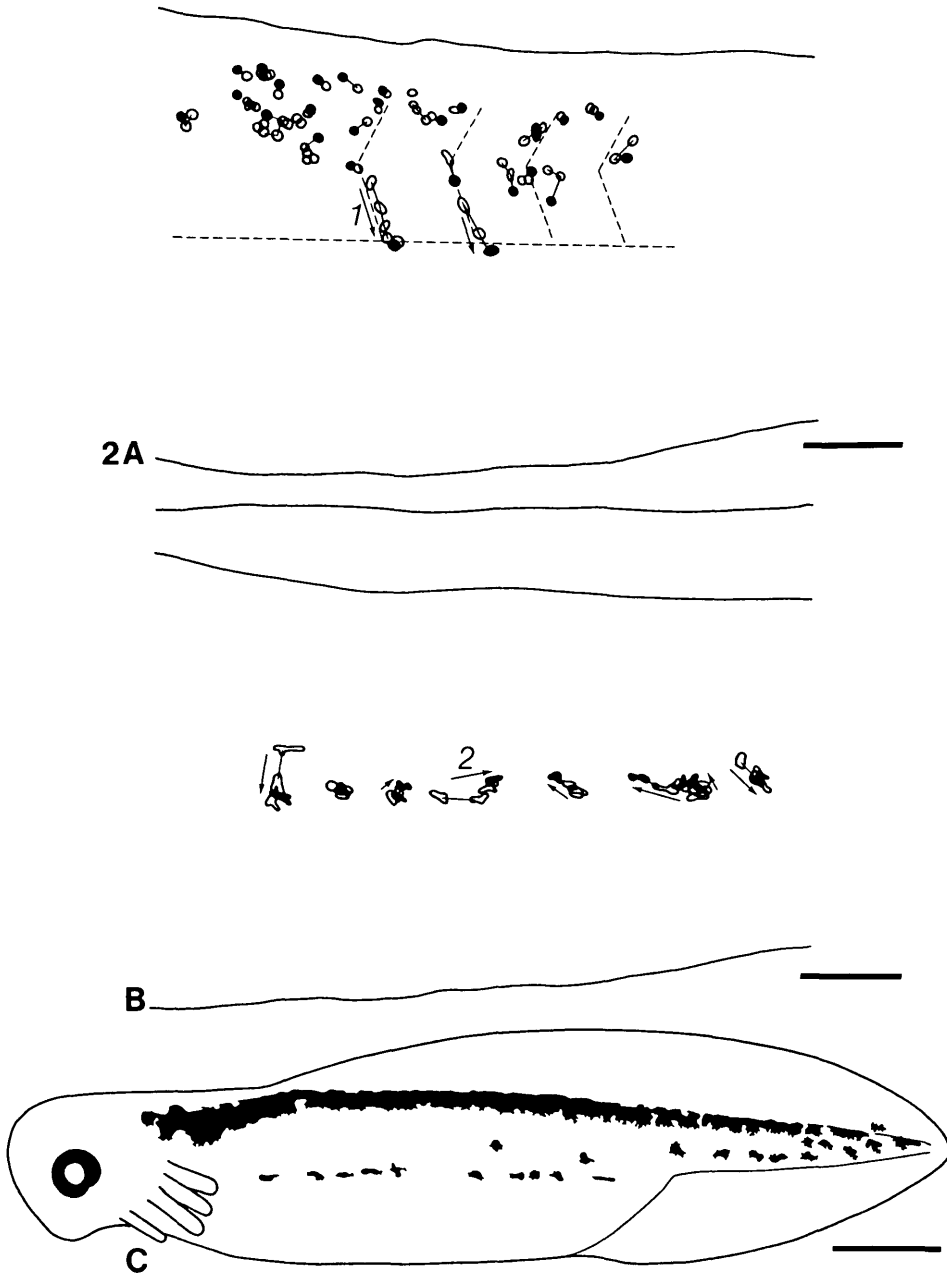


Fig. 2. (A,B) The positions of melanophores during pigment pattern formation as determined from photographs taken at 3 h intervals. Solid black cells indicate the positions of the cells in the last photograph analysed. Cells reach the somite-lateral plate mesoderm border (dashed horizontal line) by migrating along the intersomitic furrows (chevron-shaped dashed lines, A). Melanophore 1 translocated at an average rate of $0.30 \mu\text{m min}^{-1}$, melanophore 2 moved at an average rate of $0.18 \mu\text{m min}^{-1}$ (see Fig. 1). Melanophores move in both directions along the midbody stripe (B). (C) A schematic representation of the primary melanophore pattern in *T. torosa* (stage 39). Melanophores form a dense stripe at the base of the dorsal fin, and a sparse midbody stripe at the somite-lateral plate mesoderm border. Bars, (A,B) $500 \mu\text{m}$; (C) 1 mm .

During the following 24 h, melanophores migrate rostrally and caudally within the stripe along the border of the yolk mass at rates of up to $0.18 \mu\text{m min}^{-1}$ (Fig. 2B). Once a cell joins the midbody stripe, it does not venture more ventrally over the yolk mass, nor does it migrate dorsally to join the dorsal stripe. The number of melanophores that are found in the ventral stripe at stage 39 is highly variable in different clutches of embryos. This variability appears to be related to the total number of melanophores that are found in the embryo, since animals with broad, intensely pigmented dorsal stripes tend to have the most cells in the midbody stripe as well. Occasionally an embryo will be found that totally lacks a midbody stripe. These animals invariably have thin dorsal stripes with interspersed gaps and no melanophores over the surface of the somites (see below). A sample of 20 embryos (stage 39/40) from four different clutches had an average of 13.0 ± 4.4 melanophores in the midbody stripe between the forelimb bud and the posterior end of the yolk mass.

Frequently individual melanophores are encountered over the surface of the somites between the midbody and dorsal melanophore stripes. These cells are usually, but not always, found in intersomitic furrows, and they tend to be seen in the posterior half of the trunk more frequently than in anterior regions. On average, 2.9 ± 2.3 ($n = 17$) individual melanophores are found between the stripes (stage 39/40).

A typical primary pattern (the secondary pattern forms as the larva approaches metamorphosis; see Lehman, 1950) of melanophores is illustrated in Fig. 2C.

Distribution of xanthophores and iridophores

Using NH_4OH -induced pteridine fluorescence, the distribution of xanthophores has been determined during melanophore pattern formation. Xanthophores are first seen soon after melanophores appear at stage 35. Although there is considerable variability in their number and precise distribution, these cells are generally scattered among the melanophores in the anterior half of the trunk and in the head. As the melanophores become segregated into the dorsal and midbody stripes, xanthophores are seen in the head, dorsal fin, between the melanophore stripes over the surface of the somites and among the melanophores in the midbody stripe (Fig. 3A–C). This codistribution of yellow and black pigment cells in the midbody stripe is in marked contrast to the dorsal stripe, which is completely void of xanthophores. Like melanophores, xanthophores are not seen ventral to the midbody stripe over the surface of the yolk mass.

Iridophores are found in fixed specimens viewed with oblique illumination as early as stage 35. Like xanthophores, there is considerable variation in the number and distribution of these cells from embryo to embryo. Iridophores are found aligned along the dorsal surface of the neural tube in some younger (stage 35) specimens (Fig. 4A), and in slightly older embryos (stage 35/36) iridophores are found deep within the embryo (as determined by optical sectioning) along what appears to be the ventral surface of the notochord or the dorsal aorta. Iridophores are found in the trunk of older embryos (stage 36 to 40) ventral to the midbody

melanophore stripe, especially along the ventral midline near the heart (Fig. 4B), but also scattered over (or within) the lateral plate mesoderm.

Pigment cell–tissue affinities and cell morphology in situ and in vitro

Melanophores are initially observed scattered over the somites, although they are restricted to more dorsal portions of the somites in the anterior half of the trunk. When a roughly rectangular piece of ectoderm is peeled from the side of a fixed or anaesthetized embryo with tungsten needles before stage 35, nearly all of the melanophores remain associated with the surface of the somites. During the segregation phase (stages 35 to 38), melanophores remain attached to both the overlying ectoderm and the surface of the somites (Fig. 5A,B). By the time the primary melanophore pattern has developed (stage 40), all of the melanophores remain attached to the overlying ectoderm, even those cells that are in the midbody stripe (Fig. 6A,B).

Cell morphology and cell–substratum relationships were also investigated using SEM early in the ‘segregation’ phase of melanophore pattern formation (stage 35) when the migratory substratum of the melanophores is shifting from the surface of the somites to the ectoderm. Individual melanophores were identified in the SEM from light micrographs of the specimens taken before processing for electron microscopy (e.g. Fig. 5A,B). Melanophores are highly branched cells at this stage, with their processes frequently extending 75 μm to 100 μm from the elongate cell body (Figs 7D, 8B). Melanophores are restricted to the region dorsal to the pronephric duct. The only cells that are seen in the space between the lateral plate mesoderm and the overlying ectoderm are large, rounded cells that are identical in size, shape, number and distribution to leukocytes that have been identified by the dopa-reaction and TEM in earlier studies (Tucker & Erickson, 1986c). Cells that remain on the surface of the somites are frequently aligned along the intersomitic furrows; other cells are found associated with the pronephric duct (Fig. 7B), which is located superficially beneath the ectoderm (Fig. 7A). At stage 35, the mid-lateral line placode primordium is passing between the ectoderm and the ectoderm’s basal lamina in the anterior part of the trunk approximately midway between the dorsal fin and the pronephric duct. The placode primordium displaces cells of the underlying somites to form a groove that is visible in the SEM (Fig. 7B). Melanophores frequently align along the placode primordium at this stage.

The morphology of pigment cells and their precursors changes dramatically between stages 33/34, when they are initially entering the lateral migratory pathway, and stage 36/37, when melanophores are segregating into dorsal and midbody stripes. At the onset of migration (Fig. 8A), these cells have broad lamellae and tend to be roughly rectangular in shape. In contrast, at later stages of development, melanophores tend to be elongate with many long processes (Figs 7C, 8B). Numerous filopodia are observed associated with the lateral surfaces of the long processes as well as at the tips of the processes. These tips frequently flare into a fan shape that resembles a neuronal growth cone (Fig. 8B).

Similar changes in melanophore morphology are observed when neural crest cells are maintained *in vitro*. On tissue culture plastic, neural crest cells lack long processes (Fig. 11A,B). Soon after melanization, however, melanophores develop long processes extending up to 250 μm . Xanthophores do not develop similar processes. Instead these cells remain ovoid (Fig. 9A). When cultured on collagen gels, melanophores show a similar propensity for arborization, unlike xanthophores, which remain round or fusiform (Fig. 9B).

The control of midbody stripe formation

The position of the midbody stripe coincides precisely with the location of the pronephric duct. When viewed in the SEM (Fig. 7A,B) or in thick sections (Fig. 12E), the pronephric duct is found just beneath the surface of the ectoderm from stage 34/35, when melanophores are appearing, to stage 38, when the primary pattern of melanophores is nearing completion. Furthermore, melanophores are frequently observed closely associated with the pronephric duct, especially during the early stages of pattern formation.

At stage 36/37, when melanophores are migrating caudally and rostrally along the midbody stripe, it is possible to cut a slit in the ectoderm just ventral to the pronephric duct and carefully extract the duct with tungsten needles. The melanophores that were part of the midbody stripe remain attached to the excised duct (Fig. 10A,B). This intimates that the duct (or its associated vasculature) is acting as a migratory substratum for melanophores in the midbody stripe, perhaps functioning as a trap for the melanophores dispersing ventrally along the inter-somitic furrows.

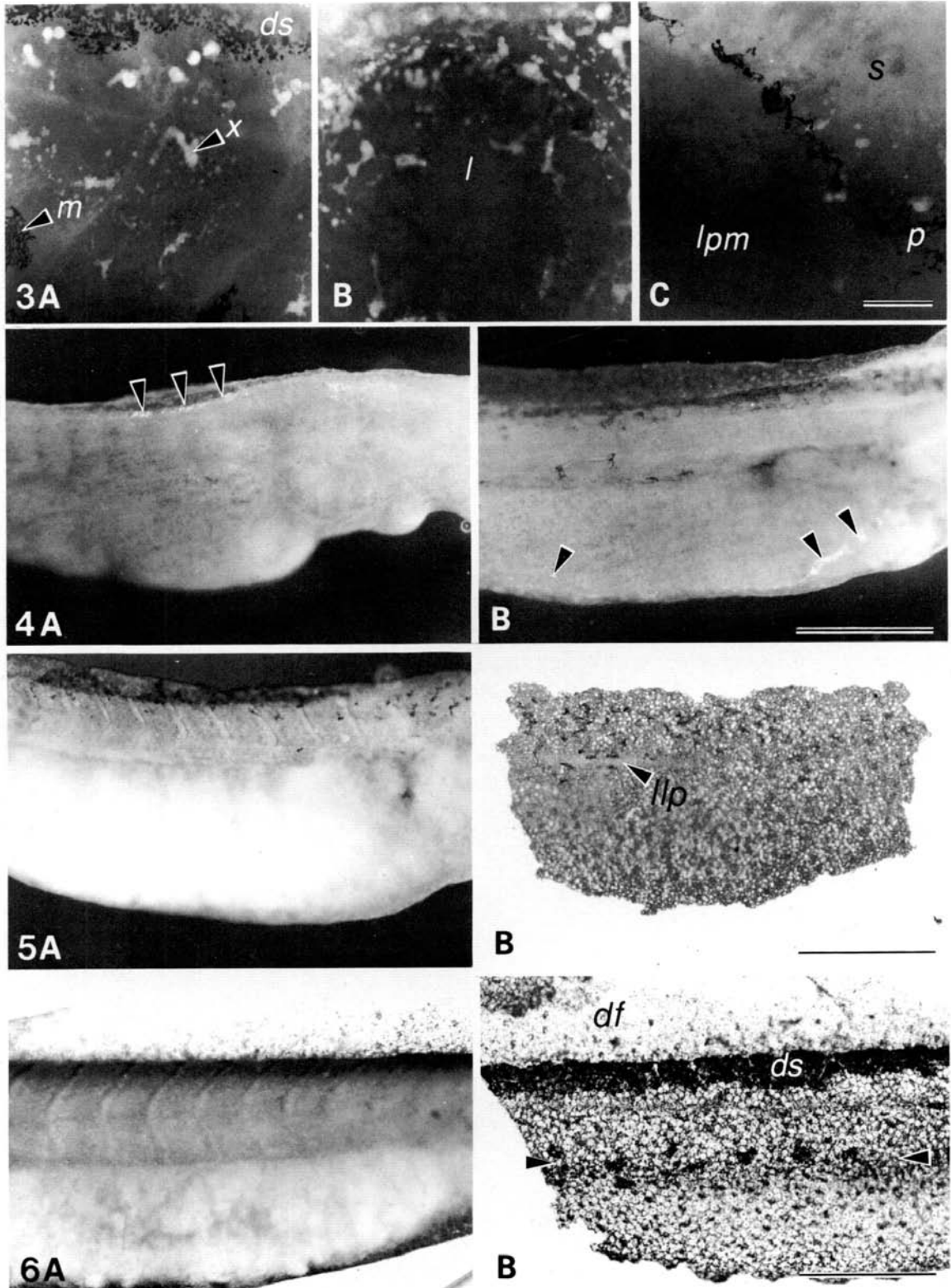
The pronephric duct is eventually internalized in an anterior-posterior wave, bringing it nearer to the dorsal aorta. Time-lapse analysis of the midbody stripe

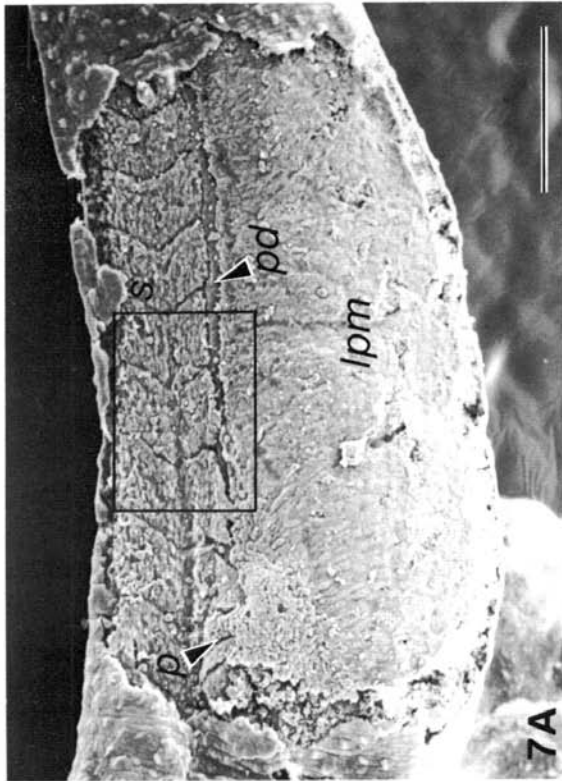
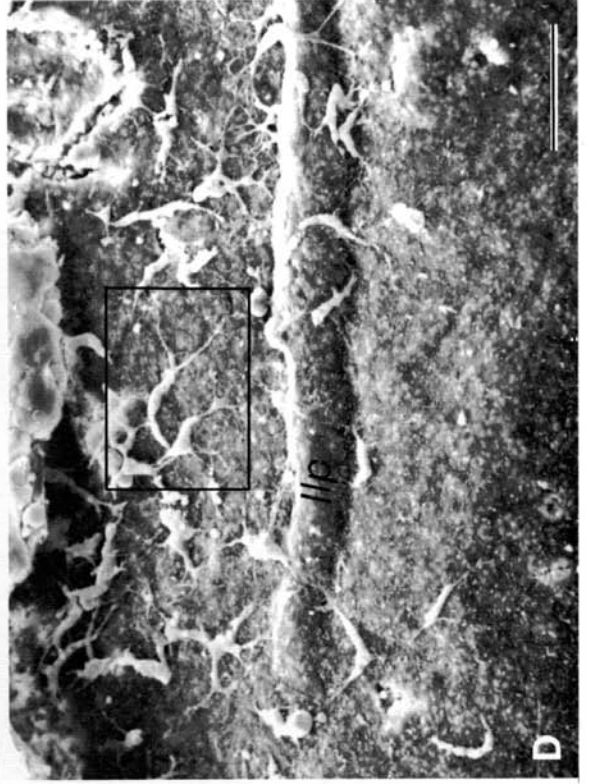
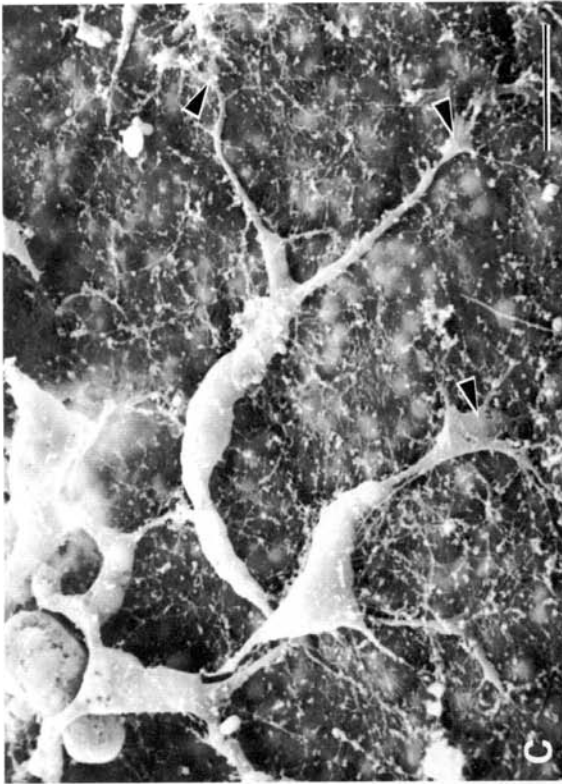
Fig. 3. The distribution of xanthophores was determined using fluorescence microscopy in stage 39 embryos. (A) Xanthophores (*x*) are found between the dorsal melanophore stripe (*ds*) and melanophores (*m*) of the midbody stripe scattered over the surface of the somites. (B) Xanthophores are also found in the head of the embryo, where there are few melanophores, especially around the developing eye (lens, *l*). (C) Xanthophores are seen in the pronephros (*p*) as well as in the midbody melanophore stripe, but not over the surface of the lateral plate mesoderm (*lpm*). Somites, *s*. Bar, 100 μm .

Fig. 4. Iridophores were identified by their luster with bright, oblique illumination. (A) Iridophores are found in a stage 35 embryo aligned along the dorsal surface of the neural tube (arrows). (B) In older embryos (stage 39/40) iridophores are found near the heart and in the lateral plate mesoderm (arrows). Bar, 1 mm.

Fig. 5. (A) When the ectoderm is peeled from a stage 35 embryo, some melanophores remain attached to the surface of the somites, however (B) many melanophores are attached to the ectoderm. The midlateral line placode primordium (*llp*) is found associated with the ectoderm in the anterior half of the trunk. Melanophores are frequently aligned along this structure. Bar, 1 mm.

Fig. 6. (A) When the ectoderm is peeled from an older embryo (stage 39/40), no melanophores remain associated with the somites. (B) Melanophores in the dorsal stripe (*ds*) and midbody stripe (between arrows) are removed with the ectoderm. The dorsal fin (*df*) does not contain melanophores. Bar, 1 mm.





during this internalization (stages 38 to 40) shows that many melanophores in the midbody stripe remain associated with the pronephric duct and are gradually lost from external view (Fig. 11A,B). This would explain why there tend to be fewer cells in the midbody stripe of older embryos than are found in the stripe during the earlier segregation phase. Melanophores that remain in the midbody stripe are firmly attached to the ectoderm (Fig. 6B).

To test directly the role of the pronephric duct in midbody stripe formation, the pronephric primordium was removed from one side of the embryo before the appearance of melanophores, and the development of melanophore patterns was observed. At stage 37, some melanophores are found ventrally over the lateral plate mesoderm on the flank without a duct (Fig. 12A,B), although most of the melanophores are distributed over the surface of the somites. At stage 38/39, there is no midbody stripe on the side of the embryo without a duct, in contrast to the unoperated side of the embryo (Fig. 12C,D). Instead, melanophores are scattered over the surface of the somites. Melanophores are no longer seen on the dorsal part of the lateral plate mesoderm as they are at earlier stages. The distribution of xanthophores was determined in one duct-ablated embryo at stage 38/39 using NH_4OH -induced fluorescence. Xanthophores, like melanophores, are found over the surface of the somites in these animals, and not over the lateral plate mesoderm.

When the experimental animals are serially sectioned, it is clear that the duct is completely removed from the right side of the embryo (Fig. 12E). The remaining duct, which has melanophores associated with it, is unusually large, perhaps to compensate for the loss of function of the missing pronephros.

Grafts to the ventral regions

Melanophore precursors were introduced into the regions ventral to the pronephric duct by grafting neural folds to a site near the ventral midline. Melanophores appear in the graft at the same time as in siblings of the donor. In

Fig. 7. Scanning electron micrographs of a stage 35 *T. torosa* embryo with the ectoderm peeled away from the trunk. (A) The pronephric duct (*pd*) can be seen ventral to the somites extending caudally from the pronephros (*p*). The lateral plate mesoderm (*lpm*) is free from cells with the characteristic morphology of pigment cells. (B) A higher magnification of the region enclosed by the box in Fig. 7A. Cells are seen aligned along the intersomitic furrows (1) and pronephric duct (*pd*; 2). The large, rounded cells found over the surface of the somites and lateral plate mesoderm (3) are probably wandering leukocytes. Cells are also aligned along the groove (*g*) formed by the passage of the lateral line placode primordium (see Fig. 7D). From bright field observation of the specimen, only two cells (*m*) in this field are known to be melanophores. (C) High magnification of the regions enclosed by the box in Fig. 7D shows two cells identified as melanophores attached to the ectoderm. These cells have long processes that end in neurite-growth-cone-like thickenings (arrows). (D) The surface underlying the ectoderm peeled away from the embryo shown in Fig. 7A, directly opposite the somitic surface shown in Fig. 7B. Approximately 75 % of the cells found attached to the ectoderm are melanophores. Most of the cells remain dorsal to the bulging lateral line placode primordium (*llp*) and many cells align along the primordium. Bars, (A) 500 μm ; (B,D) 100 μm ; (C) 25 μm .

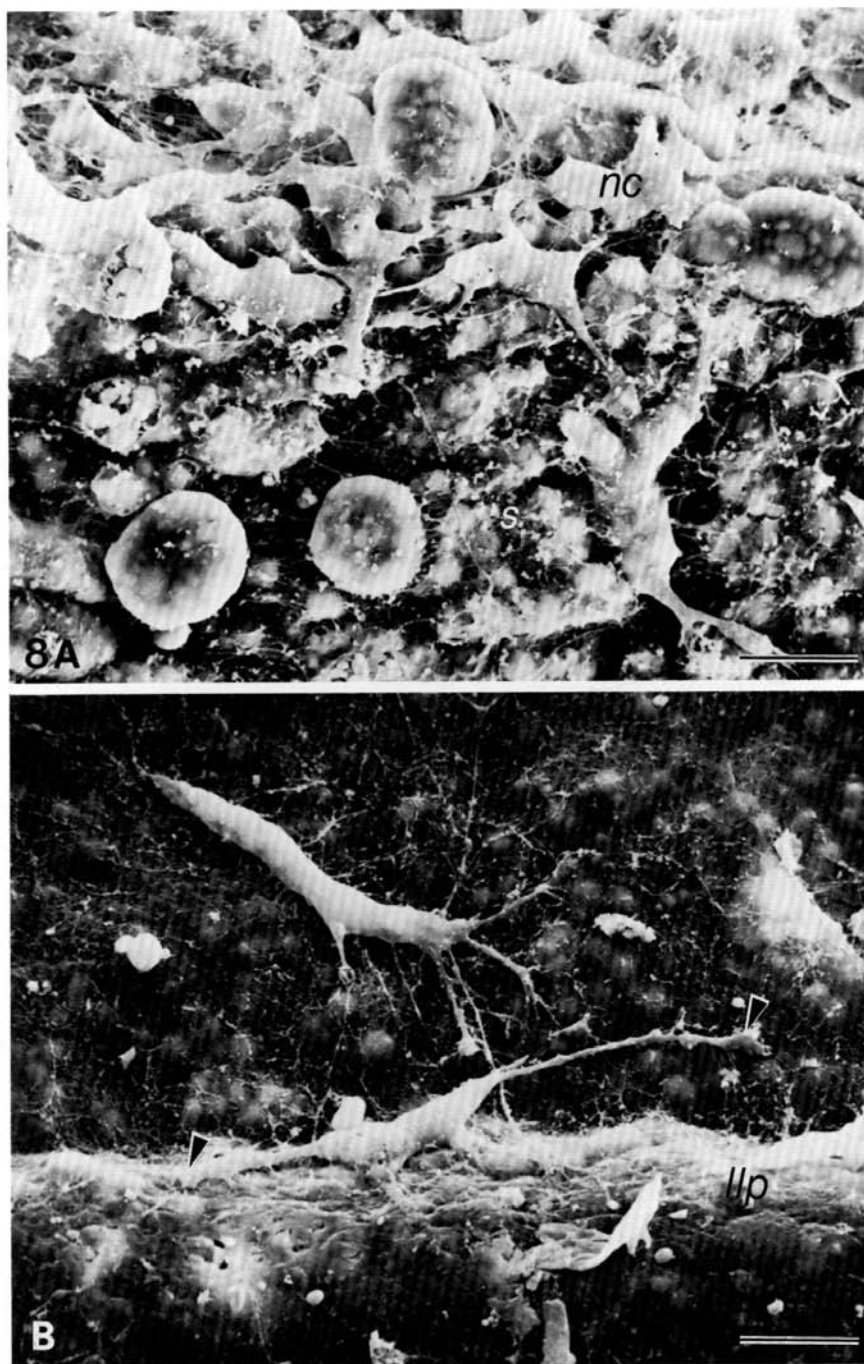


Fig. 8. (A) Neural crest cells (*nc*) entering the lateral pathway over the apex of the somites (*s*) in the posterior trunk of a stage 35 embryo. The neural crest cells lack long processes, and resemble neural crest cells in culture (Fig. 17A,B). (B) Soon after melanization, long processes (arrows) and numerous filopodia are seen extending from cells attached to the ectoderm near the lateral line placode primordium in a stage 37 embryo. Bars, 25 μ m.

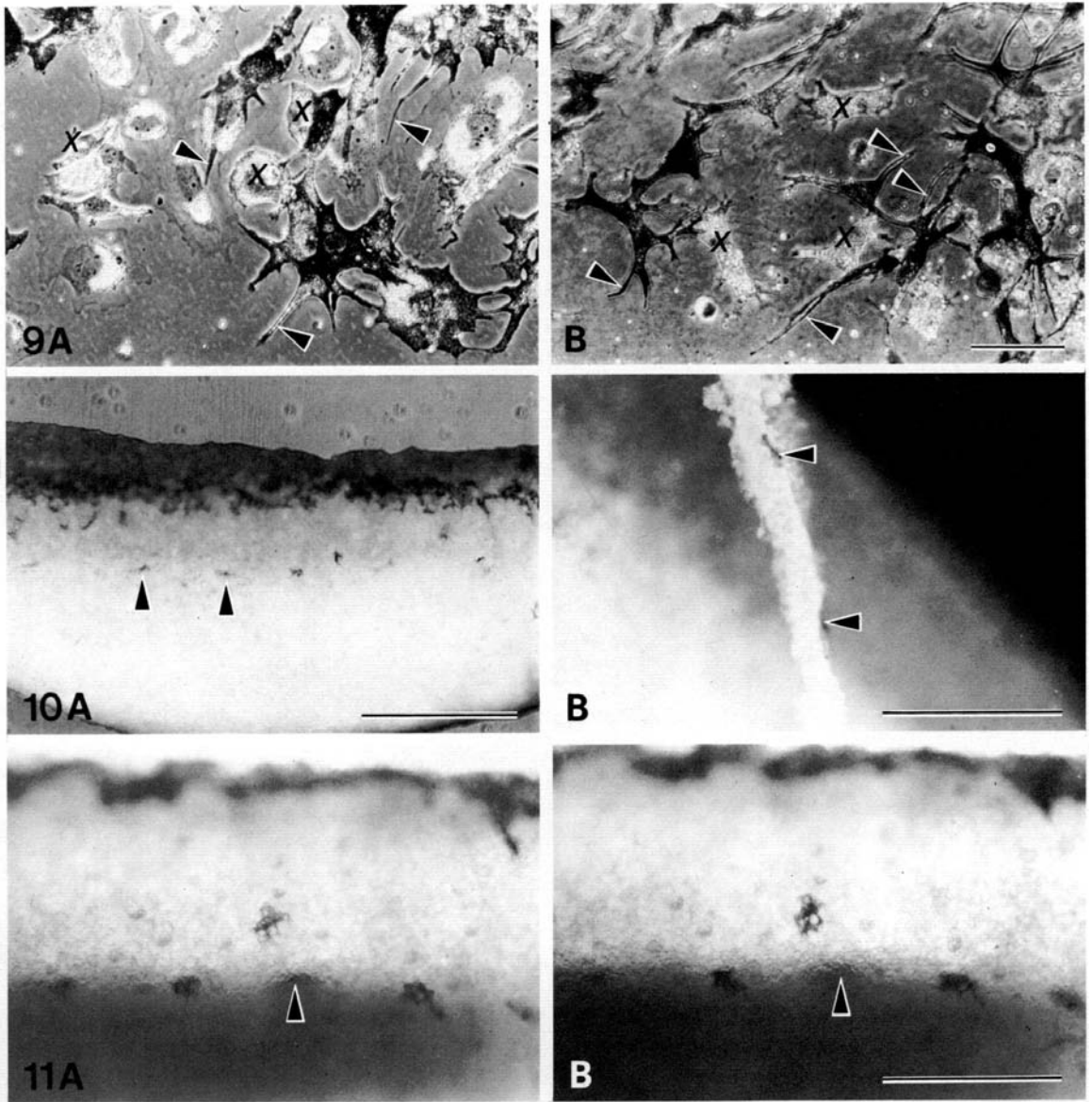
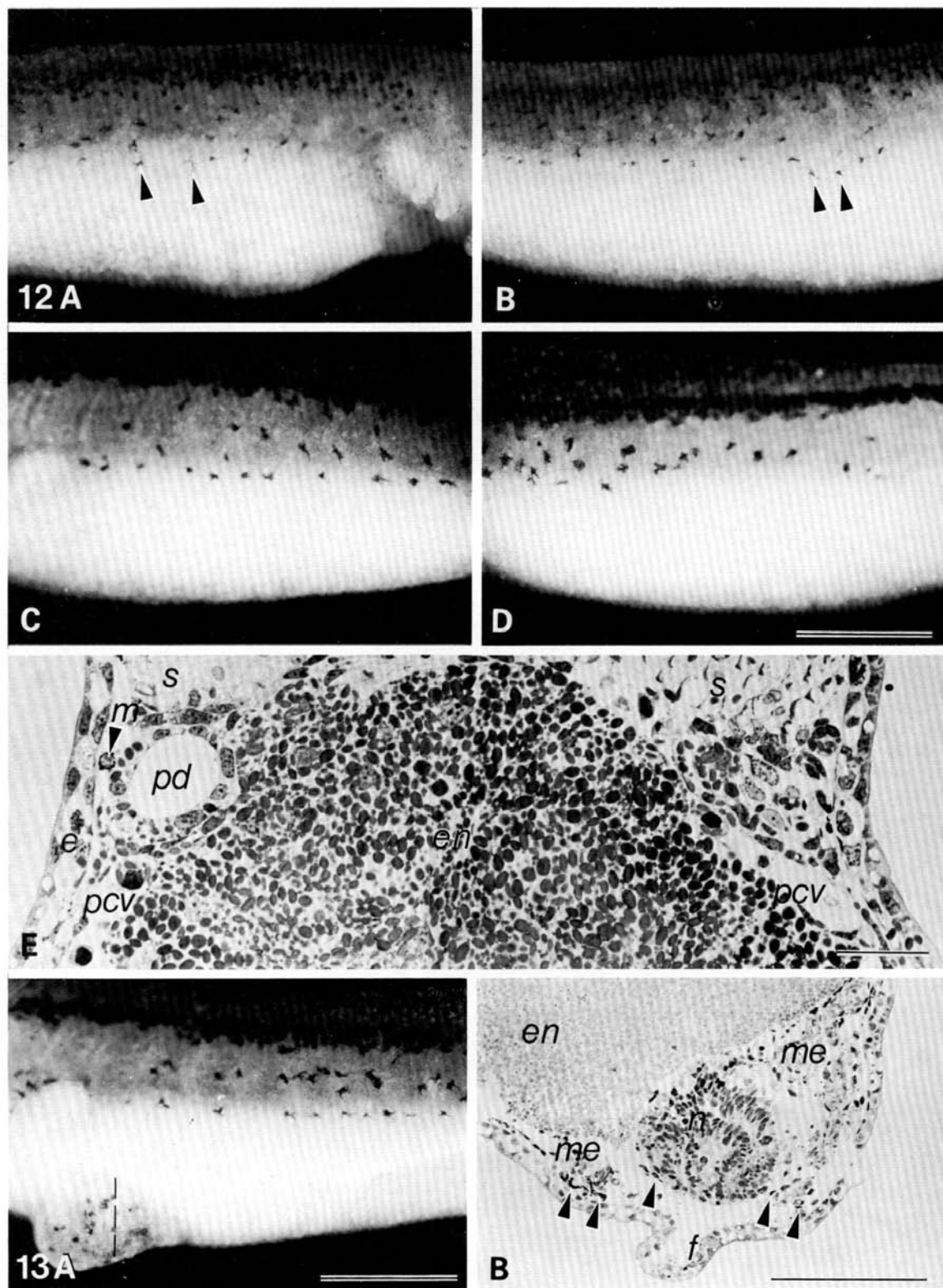


Fig. 9. The morphology of xanthophores (x) and melanophores cultured on tissue culture plastic (A) and on collagen gels (B). Xanthophores tend to be rounded or bipolar, whereas melanophores extend long processes (arrows). Bar equals 100 μ m.

Fig. 10. Melanophores in the midbody stripe (arrows, A) are attached to the pronephric duct (arrows, B) when the duct is surgically excised. Bars, (A) 1 mm; (B) 500 μ m.

Fig. 11. Two micrographs taken at a 6 h interval show a melanophore (arrow) being internalized with the pronephric duct. Note the changes in the shape but not the location of the melanophore just dorsal to the midbody stripe. Bar, 500 μ m.



one of three experiments, melanophores were observed spread along a large blood vessel that had formed at the ventral midline, but in no other cases were melanophores observed to disperse from the donor tissue (Fig. 13A). The melanophores that were associated with blood vessels were no longer visible less than 24 h after they were first observed. It was not determined if these cells died, lost their pigmentation, or migrated out of view into the opaque endoderm. Serial sections through the graft (Fig. 13B) show structures resembling a neural tube, dorsal fin and portions of somite-like mesoderm. Melanophores in the graft, like those in the normal situation, are associated with the neuronal tissue and the 'dorsal' margin of the somite-like mesoderm. There are no apparent heterogeneities at the boundaries of the grafted tissue (i.e. scar tissue) that could account for the failure of most of the pigment cells to leave the area of the graft.

Extracellular matrix in the ventral regions of the embryo

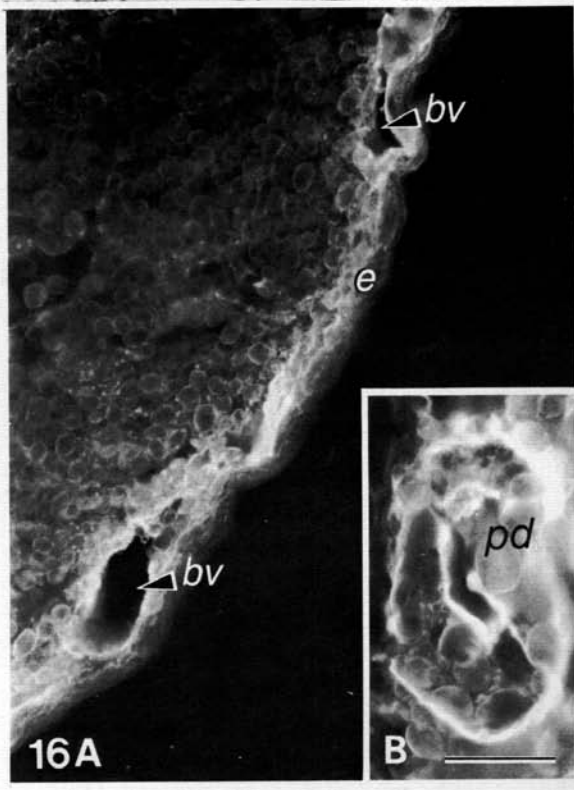
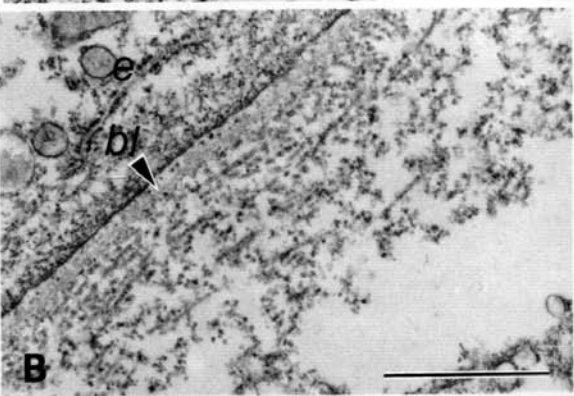
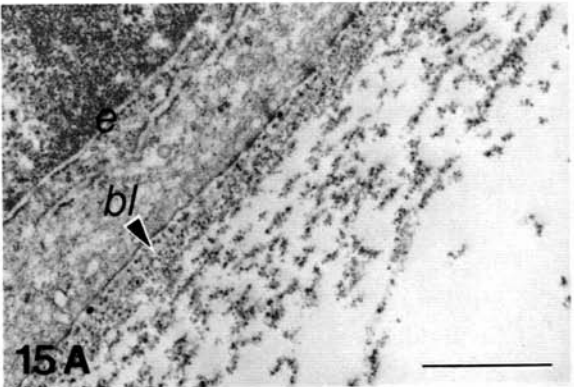
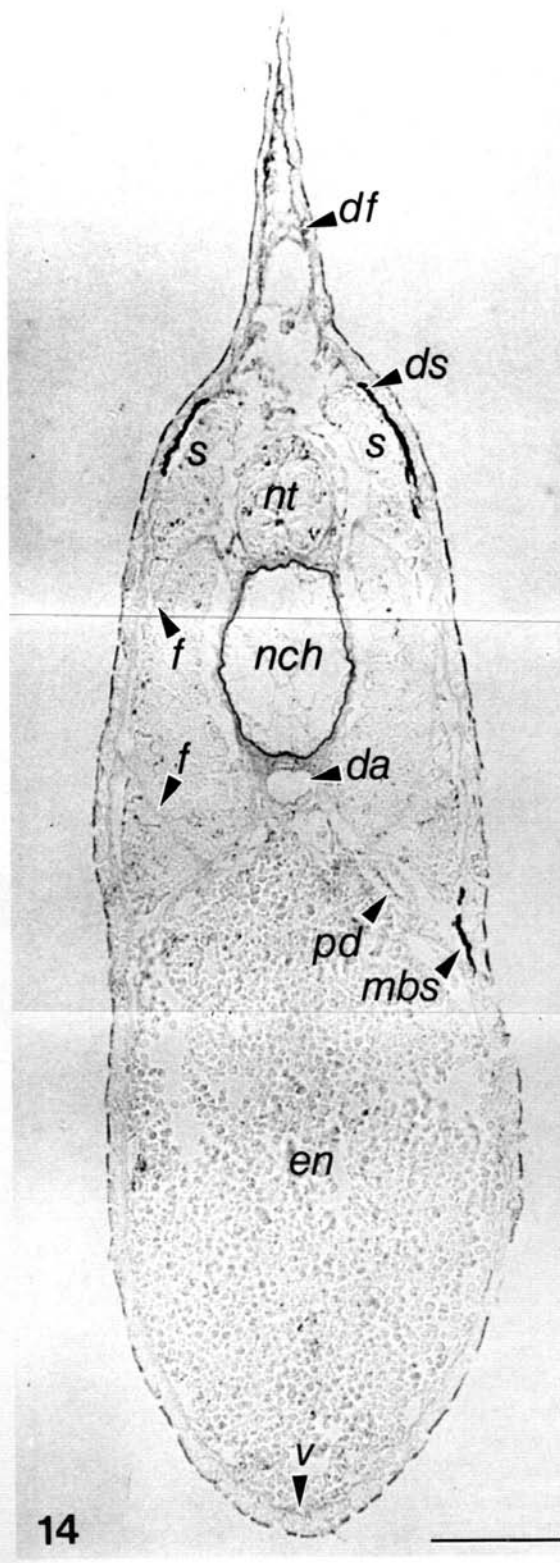
Alcian blue staining of paraffin sections reveals GAG in the dorsal fin and around the notochord, ventral neural tube, dorsal aorta and heart. However, there is relatively little staining in the spaces between the somites and the ectoderm as well as ventrally between the lateral plate mesoderm and the ectoderm (Fig. 14). This staining pattern is confirmed by observations of thin sections stained with tannic acid and ruthenium red. Striated collagen fibres coated with proteoglycan aggregates are seen to the same extent in the subectodermal ECM both dorsal and ventral to the pronephric duct (Fig. 15A,B). There is considerably less ruthenium red-positive material in the subectodermal matrix than in the tail fin ECM or near the notochord (Tucker & Erickson, 1986b). Indirect immunofluorescence reveals intense anti-FN staining around blood vessels ventral to the pronephric duct, in the ECM beneath the ectoderm dorsal and ventral to the duct, as well as around the duct itself (Fig. 16A,B).

The effect of fibronectin in vitro on cell morphology and translocation

Since FN is found along the neural crest migratory pathways during pigment cell pattern formation, we wished to determine the response of *Taricha* neural crest

Fig. 12. (A,B) In embryos (stage 37) without pronephric ducts, melanophores migrate to the dorsalmost part of the lateral plate mesoderm, but no further (arrows). (C) The unoperated side of the embryo shown in Fig. 12A,D at stage 39. Note the distinct midbody stripe. (D) The side of the embryo without a pronephric duct shown in Fig. 12C. Melanophores do not appear ventral to the somite-lateral plate mesoderm border, nor do they align to form a midbody stripe. (E) A thick section through the trunk of the embryo shown in Fig. 12C,D. There is a large pronephric duct (*pd*) on the unoperated side of the embryo that is located just beneath the ectoderm (*e*) at the base of the somites (*s*). A melanophore (*m*) is seen between the pronephric duct and the ectoderm. No duct is found on the operated side of the embryo, although the posterior cardinal vein (*pvc*) is found in its normal site. Endoderm, *en*. Bars, (A–D) 1 mm; (E) 50 μ m.

Fig. 13. (A) Melanophores do not leave donor neural fold tissue grafted to the ventral midline. (B) A section through the graft at the level indicated by the dashed line in Fig. 13A. Melanophores (arrows) are associated with somite-like mesoderm (*me*) and neuronal tissue (*n*). Endoderm, *en*; fin-like structure, *f*. Bars, (A) 1 mm; (B) 500 μ m.



cells to substrata coated with FN *in vitro*. Our analysis of the effect of FN was limited to unpigmented cells, because FN is found in the serum that must be present for *T. torosa* neural crest cells to differentiate into pigment cells in culture. Neural crest cells were cultured on tissue culture plastic in $\frac{1}{2} \times$ L-15 saline alone or $\frac{1}{2} \times$ L-15 saline with $25 \mu\text{g ml}^{-1}$ plasma FN. The presence of FN in the saline affects both cell morphology and the distance that cells spread from the neural fold explant. In the presence of FN, neural crest cells are more flattened on the substratum, with more extensive lamellipodia than cells in cultures with saline alone (Fig. 17A,B). After 13 days *in vitro*, neural crest cells migrate significantly farther ($P < 0.001$) from the edge of the explant in the presence of FN ($747 \pm 365 \mu\text{m}$, $n = 103$) than cells cultured in saline alone ($394 \pm 152 \mu\text{m}$, $n = 57$). When FN is present in the medium, the average rate of neural crest cell translocation ($0.37 \pm 0.14 \mu\text{m min}^{-1}$, $n = 10$) is not significantly different from the rate of translocation in saline alone ($0.39 \pm 0.22 \mu\text{m min}^{-1}$, $n = 7$). These rates are similar to the speed of movement of melanophores along the intersomitic furrows *in vivo* (Fig. 2A).

Contact inhibition of cell movement *in vitro*

Contact inhibition of cell movement was frequently observed in cultures of neural crest cells. Contact events were especially common and dramatic in cultures containing FN. This is apparently related to the extensive lamellipodia that form when neural crest cells are cultured on FN-coated substrata (Fig. 17A,B). When lamellipodia from two cells touch one another, ruffling of the lamellae ceases (contact paralysis). Soon after, the lamellipodia pull away from one another, and protrusive activity commences elsewhere (Fig. 18A–F). This usually results in the cells that have just collided moving away from the site of contact.

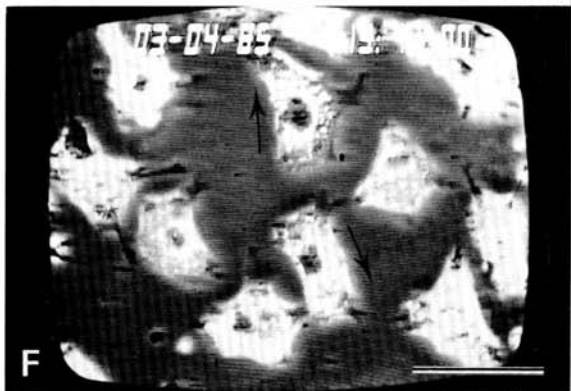
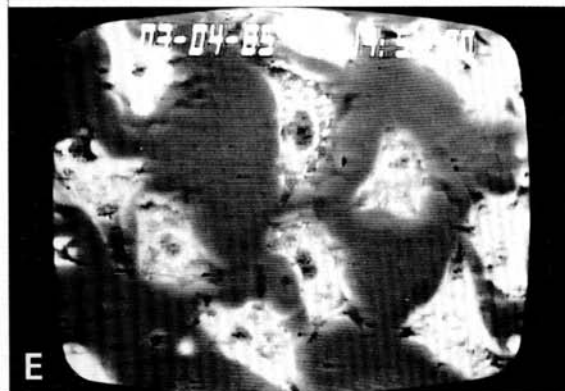
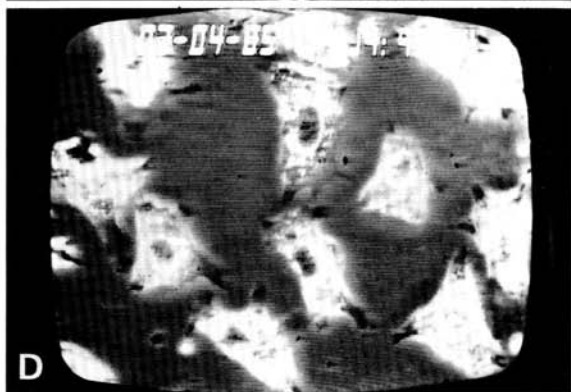
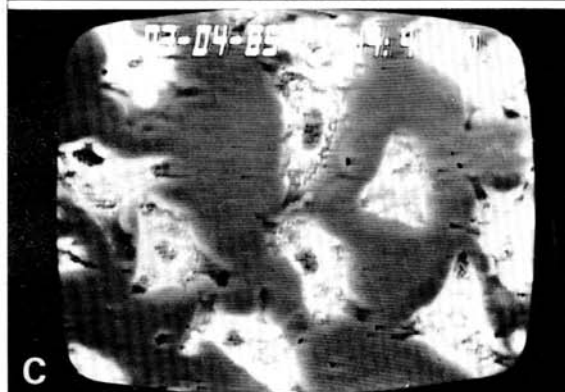
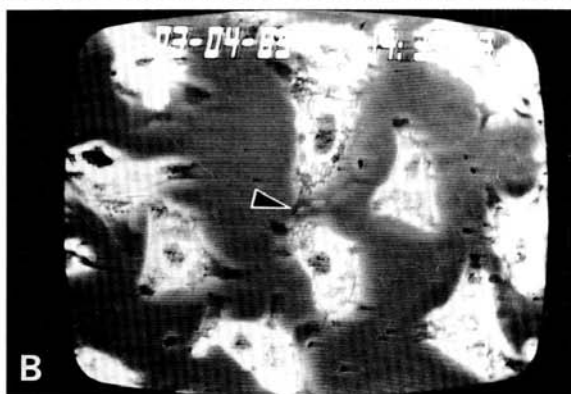
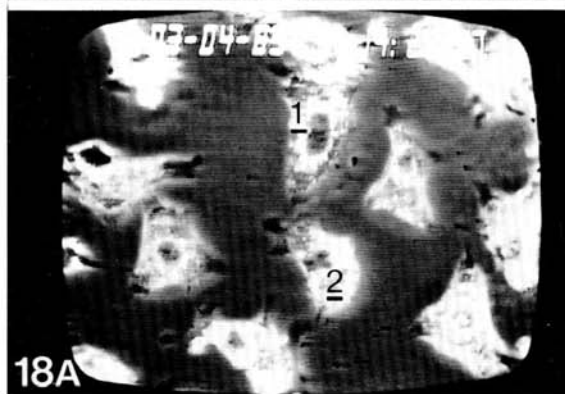
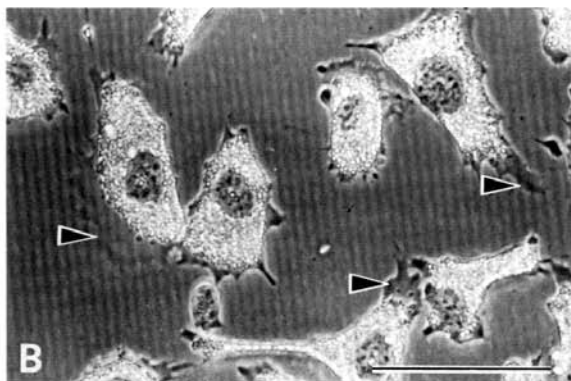
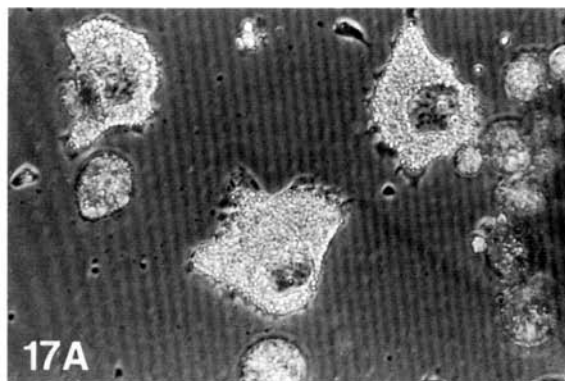
DISCUSSION

A number of mechanisms probably contribute to the development of pigment cell patterns in the embryos and larvae of *Taricha torosa*. Potential regulatory

Fig. 14. A paraffin section through the anterior trunk of a stage 39/40 embryo stained with alcian blue. There is staining of the ECM of the dorsal fin (*df*), near the ventral surface of the neural tube (*nt*), and around the notochord (*nch*) and dorsal aorta (*da*). There is also staining deep within the intersomitic furrows (*f*) and at the ventral midline (*v*). There is relatively little staining between the somites (*s*) and ectoderm, as well as in the sub-ectodermal matrix ventral to the pronephric duct (*pd*). Melanophores can be seen in the dorsal stripe (*ds*) and midbody stripe (*mbs*). Endoderm, *en*. Bar, $100 \mu\text{m}$.

Fig. 15. TEM of an embryo stained with ruthenium red and tannic acid. The ECM underlying the ectoderm (*e*) is similar ventral (A) and dorsal (B) to the pronephric duct. Proteoglycan aggregates coat the striated collagen fibres. Basal lamina, *bl*. Bars, $1 \mu\text{m}$.

Fig. 16. (A) Indirect immunostaining with anti-fibronectin antibodies stains the lateral plate mesoderm just beneath the ectoderm (*e*) as well as blood vessels (*bv*). (B) The pronephric duct is stained with anti-FN antibodies. Bar, $50 \mu\text{m}$.



mechanisms include: contact inhibition of cell movement, contact guidance, mechanical obstruction and differential adhesion. Control of pathways of cell migration, but not regional control of cell differentiation, can account for nearly all aspects of pigment cell pattern formation. However, at least one aspect of this pattern formation apparently involves the control of pigment cell differentiation. Hyaluronate inhibits the differentiation of *T. torosa* melanophores *in vitro* (Tucker & Erickson, 1986a,b). Since the dorsal fin, which at stage 40 contains melanoblasts but not melanophores (Tucker & Erickson, 1986b,c), is rich with hyaluronate (Tucker & Erickson, 1986b), the fin ECM may affect pigment cell patterning in part by inhibiting differentiation. It is important to remember, however, that this control may be acting by delaying the expression of a phenotype and not by altering the phenotypic fate of a pigment cell precursor. In urodeles, the phenotype of a pigment cell appears to be determined before the cell migrates from the dorsal surface of the neural tube (Epperlein & Löfberg, 1984).

Control of neural crest cell dispersal

The amphibian neural crest initially appears as a compact cord of cells in a groove in the dorsal surface of the neural tube. These cells disperse from their site of origin by migrating laterally over the surface of the somites, dorsally into the expanding dorsal fin and ventrally into the space between the somites and the neural tube (MacMillan, 1976; Löfberg, Ahlfors & Fällström, 1980; Tucker, 1986). What controls the directed dispersal of the neural crest into the surrounding ECM? Twitty (1944, 1953) and Twitty & Niu (1948, 1954) approached this question in *T. torosa* by culturing melanophores in capillary tubes and beneath glass coverslips. In the capillary tubes, two melanophores tended to move away from one another; when translocating beneath a coverslip, melanophores would migrate farther than surrounding cells that were not covered. They concluded that this behaviour was the result of negative chemotaxis, which is the directed migration of cells away from high concentrations of a diffusible factor produced by the pigment cells themselves. Thus, the restricted spaces of a capillary tube or beneath a coverslip are analogous to the neural crest migratory spaces *in vivo*, where pigment cells would move away from their site of origin (i.e. the site where the factor is at its highest concentration). Recent attempts to repeat these experiments with avian melanophores and freshly isolated neural crest cells have been unsuccessful (Erickson & Olivier, 1983). Since we did not observe the formation of a 'no man's land' between colliding outgrowths of *T. torosa* unpigmented neural crest or pigment cells as would be predicted by negative chemotaxis (Oldfield,

Fig. 17. *T. torosa* neural crest cells on tissue culture plastic after 13 days *in vitro*. (A) In saline alone, the cells are rounded. (B) In the presence of $25 \mu\text{g ml}^{-1}$ fibronectin, the cells appear more spread and send out extensive lamellipodia (arrows). Bar, $100 \mu\text{m}$.

Fig. 18. (A–F) Time-lapse recordings of neural crest cells *in vitro* exhibiting contact inhibition of cell movement. Lamellae extending from the cells labelled 1 and 2 make contact (arrow, B). The lamellae then contract away from the site of contact, resulting in the cells moving away from one another (arrows, F). Bar, $100 \mu\text{m}$.

1963), another mechanism may be responsible for the migration of neural crest cells away from the neural tube over the surface of the somites.

A second possible mechanism for directing the outgrowth of neural crest cells is contact guidance (Weiss, 1945). Löfberg *et al.* (1980) have reported that collagen fibres tend to be aligned parallel to the direction of neural crest cell movement in the lateral pathway and that these fibres may direct cell migration in this space. Spieth & Keller (1984), however, report evidence that collagen fibres may be aligned by traction produced by the advancing cells themselves. In fact, our results show ECM fibres aligned at a right angle to the direction of dispersal in *T. torosa* (Fig. 8A) when the neural crest is beginning to disperse and in the chick embryo ECM fibrils are frequently arranged normal to the direction of neural crest migration (Tosney, 1982).

A third possible mechanism is contact inhibition of cell movement. Keller & Spieth (1984) observed contact inhibition between axolotl neural crest cells *in vitro*, but discounted this as a possible dispersal mechanism *in vivo* (except at the earliest phases of migration) since there were not enough cells in the lateral pathway to make contact events likely. As in the axolotl and *Triturus alpestris* (Epperlein, 1974), *T. torosa* neural crest cells display contact inhibition of cell movement *in vitro* on plastic substrata. In contrast to the situation reported by Keller & Spieth (1984), however, there are numerous cells in the lateral spaces of *T. torosa* and these cells are usually close enough to another cell for contact to occur (Fig. 7B–D).

Dorsal stripe formation

Pigment cell precursors initially disperse ventrally in the lateral pathway. Soon after melanization, however, many of these cells reverse their direction of migration and translocate dorsally toward the apex of the somites to form the dorsal melanophore stripe. Thus, we are confronted with three questions. What is responsible for this change of orientation? Why are xanthophores excluded from the dorsal stripe? What is the nature of the cue that signals the cells to stop at the apex of the somites?

Twitty (1936) determined by a series of grafting experiments that the cue for dorsal stripe formation was associated with the somites themselves. When pieces from the dorsal portion of the somites were grafted ventrally with the neural tube, neural crest and overlying ectoderm, melanophores still aggregated along the somites. If somites were missing from the graft, the melanophores did not form a distinct stripe in the donor tissue. To explain the reversal of melanophore orientation in the lateral pathway, Twitty (1945) likened the situation to the clumping of *T. torosa* melanophores *in vitro*. He concluded that stripe formation was the result of melanophores pulling themselves together *via* connecting (possibly anastomosing) processes. There are only passing references to xanthophores in these early reports, and their possible interactions with melanophores were not discussed. Our observations of melanophores *in situ* and *in vitro* do not support the notion that melanophores aggregate to form the dorsal stripe by

clumping. In fact, clumping is observed only after several weeks in culture, long after the development of the dorsal stripe in the larva that provided the neural folds for culture.

There are two conspicuous changes that take place *in situ* at the time when the direction of melanophore migration changes: the migratory substratum shifts from the surface of the somites to the ECM underlying the ectoderm (as evidenced from the ectoderm-peel experiments) and recently differentiated melanophores become dendroid. The shift of migratory substratum is probably a response to increasing adhesivity of the subectodermal ECM. Throughout early development, collagen fibres are being incorporated into the dermal ECM. An increase in the number of collagen fibres or an ECM molecule associated with the fibres (such as FN, to which neural crest cells adhere tenaciously) could account for the change in substratum affinity. Unlike the somite cells in *Xenopus*, which acquire an enveloping basal lamina as the melanophores are migrating (Tucker, 1986), there is no basal lamina around the somite cells of *T. torosa* until well after the development of the primary pattern. Thus, it would be unlikely that the somite surface would be as adhesive as the dermal ECM. If the dorsal stripe cue is associated with the dermal ECM, as is suggested by ectoderm grafting experiments (Tucker & Erickson, 1986b), then this change in substratum affinity could contribute to a change in the direction of cell migration by bringing the cells in contact with a haptotactic cue. Directional migration would also be facilitated by changes in cell shape. The elongate processes that extend from melanophores *in vitro* and *in situ* frequently resemble neurite growth cones, which may find appropriate targets by haptotaxis (Nardi, 1983). It is possible that the development of long processes could lead to the change of direction of locomotion by permitting direct contact with the more adhesive substrata near the apex of the somites.

This latter hypothesis is also a possible explanation for the mechanism of xanthophore-melanophore segregation over the surface of the somites. *In vitro*, xanthophores lack long processes. If xanthophores also tend to lack long, 'searching' processes *in vivo*, these cells would be less likely to recognize the cue used by melanophores to form the dorsal stripe. The morphology of xanthophores *in situ* was not examined in detail in this study. Occasionally elongate xanthophore processes were visible using NH_4OH fluorescence, but most cells examined in this way were rounded. The destructive nature of this technique (see Materials and Methods) did not permit further ultrastructural analysis of xanthophores.

We have proposed that contact inhibition of cell movement may be responsible for the initial directed migration of neural crest cells away from the neural tube. Nevertheless, neural crest-derived melanophores eventually reverse their direction of migration and aggregate near their point of origin, the neural tube. Melanophores, unlike unpigmented neural crest cells and xanthophores observed in culture, have greatly reduced lamellipodia. Their stellate morphology and reduced lamellipodia undoubtedly contribute to a reduction in contact inhibition amongst the melanophores. Changes in the cell surface that accompany differentiation may also lead to reduced contact inhibition. Xanthophores in culture do

have lamellipodia. If these cells continue to display contact inhibition of cell movement after differentiation, this may inhibit a similar aggregation of the yellow pigment cells *in situ*.

The cue used by the melanophores to form the dorsal stripe is possibly produced by the somites (Twitty, 1936), but the cue is located in the subectodermal ECM since melanophores will form a stripe under ectoderm grafted ventrally over the lateral plate mesoderm (Tucker & Erickson, 1986b). The GAG identified in the lateral pathway using alcian blue staining and TEM appears to be homogeneous over the surface of the somites. More research is needed to identify the molecular nature of the dorsal stripe cue.

Midbody stripe formation

Why do melanophores and xanthophores stop and align at the somite–lateral plate mesoderm border in *T. torosa*? Twitty (1936) speculated that melanophores halted to form a midbody stripe due to the extreme angle that the lateral pathway takes as the ectoderm begins to surround the bulging yolk mass. From grafting experiments, Twitty (1936) also believed that some factor ventral to the somites inhibited either melanophore differentiation or migration. Our results suggest that melanophores are trapped in the lateral pathway by the pronephric duct. Melanophores reach the site of the midbody stripe by migrating through the intersomitic furrows, which apparently direct the cells ventrally as well as provide a pathway of least resistance beneath the bulging lateral line placode primordium. At the base of the intersomitic furrow, melanophores (and probably xanthophores) turn and migrate either anteriorly or posteriorly along the midbody stripe. These cells do not leave the midbody stripe to continue migrating ventrally or to return dorsally, suggesting that they are migrating on a particularly adhesive substratum (Figs 1B–D, 2B). This substratum is the pronephric duct. When the pronephric duct is surgically removed at this stage, melanophores in the midbody stripe are attached (Fig. 10A,B), and in serial sections, these cells are closely associated with the duct (Fig. 12E). The duct is located just beneath the surface of the ectoderm when the cells arrive at the base of the intersomitic furrows (Fig. 7A,B) and when it is internalized at a later stage in development many of the melanophores in the midbody stripe remain attached (Fig. 11A,B). The pronephric duct in prehatching embryos is surrounded by a basal lamina (Tucker, unpublished observations) and it stains brightly with anti-FN antibodies (Fig. 16B). Since *Taricha* neural crest cells find FN to be an adhesive substratum *in vitro*, the presence of FN in the basal lamina surrounding the duct may account, in part, for the trapping of melanophores migrating ventrally. In fact, most of the tissues surrounded by a basal lamina in the trunk of *Taricha torosa* during melanophore patterning (e.g. the dorsal neural tube, the pronephric duct and blood vessels [see below]) have melanophores associated with them. The only exceptions are the ventral neural tube and portions of the subectodermal basal lamina. Melanophores are separated from the subectodermal basal lamina by a thick layer of collagen and GAG (Fig. 15A,B), and the ventral neural tube is also surrounded with GAG (Fig. 14).

GAG can interact with FN and inhibit its adhesive properties (Rich, Pearlstein, Weissmann & Hoffstein, 1981; Erickson & Turley, 1983; Tucker & Erickson, 1984).

Although the pronephric duct halts the ventral migration of the melanophores and xanthophores in *T. torosa*, these pigment cells do not migrate ventrally between the lateral plate mesoderm and ectoderm when the duct has been ablated. This may be due, in part, to trapping of pigment cells by the posterior cardinal vein, which develops normally at the somite–lateral plate mesoderm border in spite of the absence of the pronephric duct (Fig. 12E). Nevertheless, there does appear to be some factor ventral to the duct and posterior cardinal vein that prevents the invasion of melanophores and xanthophores, because melanophores do not leave the boundaries of tissues grafted from dorsal regions onto the lateral plate mesoderm (Twitty, 1936; Tucker & Erickson, 1986b; Fig. 13A,B), except rarely along vasculature. It is interesting to note that blood vessels in the ventral tissues, like the pronephric duct, stain intensely with antibodies to FN (Fig. 16A,B) and are surrounded by a basal lamina.

Histological examination of the quantity and organization of the GAG in the lateral pathway dorsal and ventral to the pronephric duct does not reveal notable differences (Fig. 15A,B). Our methods, however, provide only crude estimates of the composition and concentration of GAG. This aspect of the study deserves reexamination following the development of more quantitative techniques.

Distribution of iridophores

Observations of *Taricha torosa* whole mounts show iridophores along the dorsal surface of the neural tube and, in older embryos, in the eye and over the lateral plate mesoderm (Fig. 4A,B). The latter observation confirms the results of Finnegan (1955), who grafted lateral plate mesoderm with its overlying ectoderm to the dorsal surface of *T. torosa* embryos and observed numerous iridophores in the grafted tissue just after larval metamorphosis. How do iridophores reach the ventral tissues from which melanophores and xanthophores are excluded? One possibility is that iridophores migrate primarily through the ventral pathway, between the somites and neural tube, instead of through the lateral pathway over the apex of the somites. Although iridophores were not identified in the TEM in the ventral pathway, this may be due to the relative scarcity of these cells, as well as to the irregularity of their numbers and distribution from animal to animal. In one whole mount, lustrous cells were present in the ventral pathway near the notochord. Perhaps *T. torosa* iridophores, like the pigment cell precursors in *Xenopus laevis* (MacMillan, 1976; Tucker, 1986), migrate through the ventral pathway and continue ventrally along the mesoderm–endoderm border or along the coelomic face of the lateral plate mesoderm instead of between the ectoderm and mesoderm. These cells would not be trapped by the superficial pronephric duct and they would not be inhibited from migrating by a factor in the dermal ECM. Iridophores are seen dorsally near the neural tube before they begin to migrate. This suggests that these cells select the ventral pathway after they have

differentiated and that their phenotype is not determined by a factor in the ventral pathway. It would be interesting to observe iridophore behaviour *in vitro* and compare interactions between iridophores and other pigment cells with substrata composed of isolated ECM macromolecules.

We would like to thank T. J. Poole for his assistance with ablation experiments, as well as P. B. Armstrong and R. E. Keller for useful comments and advice during the course of this research. We are also grateful for the cooperation of East Bay Regional Park District. This research was supported by NIH grant PHS-DE 05630 to C.A.E. and DHHS National Research Service Award GM 07377 to R.P.T.

REFERENCES

- BAGNARA, J. T., MATSUMOTO, J., FERRIS, W., FROST, S. K., TURNER, W. A., JR, TCHEN, T. T. & TAYLOR, J. D. (1979). Common origin of pigment cells. *Science* **203**, 410–415.
- DERBY, M. A. & PINTAR, J. E. (1978). The histochemical specificity of *Streptomyces* hyaluronidase and chondroitinase ABC. *Histochem. J.* **10**, 529–547.
- DUSHANE, G. P. (1935). An experimental study of the origin of pigment cells in amphibia. *J. exp. Zool.* **72**, 1–31.
- ELSDALE, T. & BARD, J. (1972). Collagen substrate for studies on cell behaviour. *J. Cell Biol.* **54**, 626–637.
- EPERLEIN, H. H. (1974). The ectomesenchymal–endodermal interaction system (EEIS) of *Triturus alpestris* in tissue culture: Observations on attachment, migration and differentiation of neural crest cells. *Differentiation* **2**, 151–168.
- EPERLEIN, H. H. (1982). Different distribution of melanophores and xanthophores in early tailbud and larval stages of *Triturus alpestris*. *Wilhelm Roux' Arch. devl Biol.* **191**, 19–27.
- EPERLEIN, H. H. & CLAVIEZ, M. (1982a). Formation of pigment cell patterns in *Triturus alpestris* embryos. *Devl Biol.* **91**, 497–502.
- EPERLEIN, H. H. & CLAVIEZ, M. (1982b). Changes in the distribution of melanophores and xanthophores in *Triturus alpestris* embryos during their transition from the uniform to banded pattern. *Wilhelm Roux' Arch. devl Biol.* **192**, 5–18.
- EPERLEIN, H. H. & LÖFBERG, J. (1984). Xanthophores in chromatophore groups of the premigratory crest initiate the pigment pattern of the axolotl larva. *Wilhelm Roux' Arch. devl Biol.* **193**, 357–369.
- ERICKSON, C. A. (1986). Morphogenesis of the neural crest. In *Developmental Biology: A Comprehensive Synthesis* (ed. L. Browder). New York: Plenum Publishing Company (in press).
- ERICKSON, C. A. & OLIVIER, K. R. (1983). Negative chemotaxis does not control quail neural crest cell dispersion. *Devl Biol.* **96**, 542–551.
- ERICKSON, C. A. & TURLEY, E. A. (1983). Substrata formed by combinations of extracellular matrix components alter neural crest cell motility *in vitro*. *J. Cell Sci.* **61**, 299–323.
- FINNEGAN, C. V. (1955). Ventral tissues and pigment pattern in salamander larvae. *J. exp. Zool.* **128**, 453–479.
- FROST, S. K., EPP, L. G. & ROBINSON, S. J. (1984a). The pigmentary system of developing axolotls. I. A biochemical and structural analysis of chromatophores in wild-type axolotls. *J. Embryol. exp. Morph.* **81**, 105–125.
- FROST, S. K., EPP, L. G. & ROBINSON, S. J. (1984b). The pigmentary system of developing axolotls. II. An analysis of the melanoid phenotype. *J. Embryol. exp. Morph.* **81**, 127–142.
- HAY, E. D. & MEIER, S. (1974). Glycosaminoglycan synthesis by embryonic inducers: neural tube, notochord, and lens. *J. Cell Biol.* **62**, 889–898.
- HEASMAN, J., HYNES, R. O., SWAN, A. P., THOMAS, V. & WYLIE, C. C. (1981). Primordial germ cells of *Xenopus* embryos: The role of fibronectin in their adhesion during migration. *Cell* **27**, 437–447.
- HÖRDSTADIUS, S. (1950). *The Neural Crest: Its Properties and Derivatives in Light of Experimental Research*. London: Oxford University Press.

- KELLER, R. E. & SPIETH, J. (1984). Neural crest cell behavior in white and dark larvae of *Ambystoma mexicanum*: Time-lapse cinemicrographic analysis of pigment cell movement *in vivo* and in culture. *J. exp. Zool.* **229**, 109–126.
- LE DOUARIN, N. (1982). *The Neural Crest*. New York: Cambridge University Press.
- LEHMAN, H. E. (1950). The suppression of melanophore differentiation in salamander larvae following orthotopic exchanges of neural folds between species of *Amblystoma* and *Triturus*. *J. exp. Zool.* **114**, 435–464.
- LÖFBERG, J., AHLFORS, K. & FÄLLSTRÖM, C. (1980). Neural crest cell migration in relation to extracellular matrix organization in the embryonic axolotl trunk. *Devl Biol.* **75**, 148–167.
- LUFT, J. H. (1971). Ruthenium red and violet: Chemistry, purification, methods of use for electron microscopy, and mechanism of action. *Anat. Rec.* **171**, 347–368.
- MACMILLAN, G. J. (1976). Melanoblast-tissue interactions and the development of pigment pattern in *Xenopus* larvae. *J. Embryol. exp. Morph.* **35**, 463–484.
- NARDI, J. B. (1983). Neuronal pathfinding in developing wings of the moth *Manduca sexta*. *Devl Biol.* **95**, 163–174.
- OLDFIELD, F. E. (1963). Orientation behavior of chick leukocytes in tissue culture and their interactions with fibroblasts. *Expl Cell Res.* **30**, 125–138.
- POOLE, T. J. & STEINBERG, M. S. (1982). Evidence for the guidance of pronephric duct migration by a craniocaudally traveling adhesion gradient. *Devl Biol.* **92**, 144–158.
- RICH, A. M., PEARLSTEIN, E., WEISSMANN, G. & HOFFSTEIN, S. T. (1981). Cartilage proteoglycans inhibit fibronectin-mediated adhesion. *Nature, Lond.* **293**, 224–226.
- SCHRECKENBERG, G. M. & JACOBSON, A. G. (1975). Normal stages of development of the axolotl, *Ambystoma mexicanum*. *Devl Biol.* **42**, 391.
- SPIETH, J. & KELLER, R. E. (1984). Neural crest cell behavior in white and dark larvae of *Ambystoma mexicanum*: Differences in cell morphology, arrangement and extracellular matrix as related to migration. *J. exp. Zool.* **229**, 91–108.
- STEVENS, L. C. JR (1954). The origin and development of chromatophores in *Xenopus laevis* and other anurans. *J. exp. Zool.* **125**, 221–246.
- TOSNEY, K. W. (1982). The segregation and early migration of cranial neural crest cells in the avian embryo. *Devl Biol.* **89**, 13–24.
- TUCKER, R. P. (1986). The role of glycosaminoglycans in anuran pigment cell migration. *J. Embryol. exp. Morph.* **92**, 145–164.
- TUCKER, R. P. & ERICKSON, C. A. (1984). Morphology and behavior of quail neural crest cells in artificial three-dimensional extracellular matrices. *Devl Biol.* **104**, 390–405.
- TUCKER, R. P. & ERICKSON, C. A. (1986a). The behavior and morphology of urodele pigment cells *in vitro*. *Axolotl Newsletter* **15**, 7–11.
- TUCKER, R. P. & ERICKSON, C. A. (1986b). Pigment cell pattern formation in *Taricha torosa*: The role of the extracellular matrix in controlling pigment cell migration and differentiation. (Submitted.)
- TUCKER, R. P. & ERICKSON, C. A. (1986c). Pigment cell pattern formation in amphibian embryos: A reexamination of the dopa technique. *J. exp. Zool.* (in press).
- TURLEY, E. A., ERICKSON, C. A. & TUCKER, R. P. (1985). The retention and ultrastructural appearances of various extracellular matrix molecules incorporated into three-dimensional hydrated collagen lattices. *Devl Biol.* **109**, 347–369.
- TWITTY, V. C. (1936). Correlated genetic and embryological experiments on *Triturus*. I and II. *J. exp. Zool.* **74**, 239–302.
- TWITTY, V. C. (1942). The species of Californian *Triturus*. *Copeia* **1942**, 64–76.
- TWITTY, V. C. (1944). Chromatophore migration as a response to mutual influences of the developing pigment cells. *J. exp. Zool.* **95**, 259–290.
- TWITTY, V. C. (1945). The developmental analysis of specific pigment patterns. *J. exp. Zool.* **100**, 141–178.
- TWITTY, V. C. (1953). Intercellular relations in the development of amphibian pigmentation. *J. Embryol. exp. Morph.* **1**, 263–268.
- TWITTY, V. C. & BODENSTEIN, D. (1939). Correlated genetic and embryological experiments on *Triturus*. III. Further transplantation experiments on pigment development. IV. The study of pigment cell behavior *in vitro*. *J. exp. Zool.* **81**, 357–398.

- TWITTY, V. C. & BODENSTEIN, D. (1944). The effect of temporal and regional differentials on the development of grafted chromatophores. *J. exp. Zool.* **95**, 213–231.
- TWITTY, V. C. & NIU, M. C. (1948). Causal analysis of chromatophore migration. *J. exp. Zool.* **108**, 405–437.
- TWITTY, V. C. & NIU, M. C. (1954). The motivation of cell migration, studied by isolation of embryonic pigment cells singly and in small groups *in vitro*. *J. exp. Zool.* **125**, 541–574.
- WEISS, P. (1945). Experiments on cell and axon orientation *in vitro*: The role of colloidal exudates in tissue organization. *J. exp. Zool.* **100**, 353–386.
- WESTON, J. A. (1980). Role of the embryonic environment in neural crest morphogenesis. In *Current Research Trends in Craniofacial Development* (ed. R. M. Pratt & R. L. Christiansen), pp. 27–45. New York: Elsevier/North Holland.

(Accepted 22 April 1986)